Metal nanospheres under intense continuous-wave illumination: A unique case of nonperturbative nonlinear nanophotonics

I. Gurwich and Y. Sivan[*]

Unit of Electro-optics Engineering, Faculty of Engineering Sciences, Ben-Gurion University of the Negev, Israel

We show that the standard perturbative (i.e., cubic) description of the thermal nonlinear response of a single metal nanosphere to intense continuous-wave (CW) illumination is sufficient only for a temperature rise of up to 100 degrees above room temperature. Beyond this regime, the slowing down of the temperature rise requires a nonperturbative description of the nonlinear response, even though the permittivity is linearly dependent on the temperature and despite the deep subwavelength effective propagation distances involved. Using experimental data, we show that, generically, the increase of the imaginary part of the metal permittivity dominates the increase of the host permittivity as well as the resonance shift due to the joint changes to the real parts of the metal and host. Thus, the main nonlinear effect is a decrease of the quality factor of the resonance. We further analyze the relative importance of the various contributions to the temperature rise and thermal nonlinearity, compare the nonlinearity of Au and Ag, demonstrate the potential effect of the nanoparticle morphology, and show that although the thermo-optical nonlinearity of the host typically plays a minor role, its thermal conductivity and its temperature dependence is important. Finally, we discuss the differences between CW and ultrafast thermal nonlinearities.

I. INTRODUCTION

Nonlinear optical effects are usually weak. For example, typical second-order nonlinear processes have efficiencies of only a few percent for nonlinear crystals a few millimeters in length [1]. Third-order nonlinear effects are usually weaker and occur on even longer distances; see, for example, self-phase modulation in optical fibers [2] or even in highly nonlinear semiconductor waveguides [3]. Even the relatively strong *slow* nonlinearities, which give rise to permittivity and refractive index changes, are usually limited to modest values due to saturation effects (see Ref. [4] and references therein), phase transitions (e.g., in liquid crystals), or damage (e.g., in photorefractive materials). Accordingly, the vast majority of theoretical studies of nonlinear optical effects are performed within the framework of a perturbative description, i.e., involving, at most, a third-order (equivalently, cubic) nonlinearity. This is true, in particular, on the nanoscale, where the relevant propagation distances can be below the wavelength scale.

Recently, the need to go beyond the perturbative description was demonstrated experimentally in near-zero permittivity films, a few hundreds of nanometers thick, under ultrafast illumination [5–7]. However, a *much stronger nonlinear response* was observed in a recent measurement of scattering of intense beams from *single metal nanoparticles* [8–12]. These measurements, although being conceptually simple, differed considerably with respect to the many previous measurements of nonlinear scattering from metal nanostructures (see, e.g., Refs. [13–18], to name just a few) and, in particular, with respect to Refs. [5–7]. First, they employed intense *continuous wave* (CW) light rather than the usual ultrafast illumination. Second, they relied on a confocal microscope rather than the usual Z-scan measurements (and their variations). Third,

they were taken from *single nanoparticles* rather than from composites or uniform films. Thus, a theoretical description of the results of Refs. [8–12] requires a nonperturbative description at much lower intensities, without a vanishing permittivity, and in substantially smaller volumes, below the wavelength scale.

In Ref. [19] it was shown that the thermal effect, known to be among the strongest mechanisms of optical nonlinearity [1], enables one to reproduce *qualitatively* the experimental results of nonlinear scattering from Au nanoparticles [8–12] for moderately high intensities. In the current article, using the best experimental data available for the temperature dependence of the permittivities, as well as numerical simulations and an approximate analysis, we go beyond Ref. [19] and study the nonlinear scattering from a *single* metal nanoparticle systematically and quantitatively, with the dual aim of demonstrating the failure of the perturbative (cubic) description as well as classifying the importance of the various contributing physical effects. Specifically, we compare the nonlinear scattering from Au and Ag nanoparticles; we study also the possible contribution of the optical properties of the dielectric host to the overall nonlinear response and show that in the absence of a phase transition (e.g., boiling) of the host, they have a relatively smaller role compared to that of the optical properties of the metal; this justifies, a posteriorly, the neglect of the host nonlinearity in Ref. [19]. We also show that, quite unintuitively, changes of the real part of the metal permittivity have generically a secondary effect on the temperature and field. Further, we demonstrate qualitative differences related with the sphere morphology, as well as with the thermal properties of the dielectric host. Throughout the study, we elucidate the differences between the strength of the thermal nonlinearity in the ultrafast and CW cases. This is important because while the former is well studied, the latter, i.e., the CW case, has been practically ignored; see discussion in Ref. [19].

———————
[*]sivanyon@bgu.ac.il

This study provides an important step towards reaching a quantitative understanding of the nonlinear scattering of CW light observed in Refs. [8–12] (i.e., matching theoretical predictions to the experimental data) by identifying which physical effects are most relevant. Since many of the relevant material parameters are not known (e.g., the temperature dependence of the thermal conductivity of the host, the Kapitza resistance of the various metal-dielectric combinations and its temperature dependence, etc.), this study also shows which effect deserves an elaborate quantification. It also allows us to suggest experiments that can provide further support to our claims on the dominance of the thermal effects.

The paper is organized as follows. In Sec. II, we describe the basic assumptions of the model, and in Sec. III we develop the model equations for the temperature, permittivity, and field within the nanosphere. We then proceed by several numerical examples (Sec. IV) and complement the numerical results with an approximate analysis (Sec. V). Section VI provides a discussion of the results and an outlook.

II. MODEL ASSUMPTIONS

In what follows, we denote the quantities within the metal nanosphere (host) with a subscript m (h); we also label the ambient properties by a subscript 0.

The physical configuration studied in the current article is of a single metal nanosphere in a dielectric host under intense CW illumination. We consider spheres which are sufficiently small so the incident and total field as well as the temperature within the metal nanosphere (E_{inc}, E_m, and T_m, respectively) can be approximated as being uniform [20]. The former assumption, known as the quasistatic approximation, is justified for particles sufficiently small with respect to the wavelength; the latter is valid when the host has a relatively low thermal conductivity compared with the sphere (i.e., $\kappa_h \ll \kappa_m$) [19,21,22].

We further assume that the nanospheres exhibit only linear (one-photon) absorption. While we do not expect multiphoton absorption to yield anything more than a quantitative change to the results shown below, it is also worth noting that the absorption cross sections of multiphoton processes are difficult to distinguish from the many other effects (e.g., the thermal effect, free-carrier generation, stress or strain, etc.) and are in general not well characterized and, hence, difficult to quantify at this stage.

Under these assumptions, it was shown in Ref. [19] that an *exact* solution of the coupled Maxwell and heat equations is available, whereby the temperature inside a few nm sphere is given by

$$\Delta T \equiv T_m - T_{h,0} = \frac{a^2}{3\kappa_h(T)} p_{\text{abs}}(T),$$
$$p_{\text{abs}}(T) \equiv \frac{\omega}{2}\epsilon_0 \epsilon_m''(T)|\vec{E}_m|^2, \qquad (1)$$

where a is the sphere radius, ω is the angular frequency of the incoming photons, ϵ_0 is the vacuum permittivity, and where

$$\vec{E}_m = \frac{3\epsilon_h(T)}{\epsilon_{\text{tot}}'(T) + i\epsilon_m''(T)} \vec{E}_{\text{inc}}, \qquad (2)$$

is the field inside the nanosphere, $\vec{E}_{\text{inc}}$ is the incident field amplitude, and $\epsilon_{\text{tot}}'(T) \equiv 2\epsilon_h(T) + \epsilon_m'(T)$. This solution is based on the fact that, in this limit, the functional form of the field and temperature are known exactly (specifically, without neglecting reflection etc.). Thus, the only remaining unknown, their level, can be determined by simple ("fixed-point") iterations.

In order to compute the field and temperature, we now need to specify the temperature dependence of the various parameters (i.e., the various thermoderivatives). Since we want to focus on the interplay among the field, temperature, and various thermoderivatives, we avoid dwelling into the detailed solid-state physics aspects of the metal permittivity and its temperature dependence (see, e.g., Refs. [13,23–25]). Instead, we rely on the best available empirical data. Specifically, we assume a linear dependence of the permittivity on the temperature, namely

$$\epsilon_m(T) = \epsilon_{m,0}' + \frac{d\epsilon_m'}{dT}\bigg|_{T_{h,0}} (T - T_{h,0})$$
$$+ i\left[\epsilon_{m,0}'' + \frac{d\epsilon_m''}{dT}\bigg|_{T_{h,0}} (T - T_{h,0})\right], \qquad (3)$$

where $T_{h,0}$ is the ambient temperature of the host (i.e., away from the nanosphere). This was shown to be the case at least up to several hundreds of degrees in recent ellipsometry measurements of Au thin films [26,27]; the data in these studies were remarkably similar and in excellent agreement with an earlier study [28] performed over a narrower temperature range. Similar linear dependence on the temperature for a Ag film can be deduced from the model derived in Ref. [24] by extracting the dependence of the permittivity on the electron and lattice temperatures from transient spectroscopy measurements of thin Ag films under an ultrafast illumination [29]; this paper describes probably the most detailed study, to date, of the temperature dependence of the Ag permittivity (in terms of wavelength and temperature range). An ellipsometry study of thin Ag films (which appeared after the submission of this article) reports similar results [30].

Similarly, we assume for the host media that $\epsilon_h = \epsilon_{h,0}' + d\epsilon_h'/dT|_{T_{h,0}}(T - T_{h,0})$ (see, e.g., data in Ref. [1]) and that its thermal conductivity varies linearly with temperature, i.e., $\kappa_h = \kappa_{h,0} + d\kappa_h/dT|_{T_{h,0}}(T - T_{h,0})$. Under the above assumptions, the thermal conductivity can also account for the temperature dependence of the Kapitza resistance via a slight modification of the solution (1) [19,31].

For brevity, in what follows, we denote $B_m \equiv d\epsilon_m/dT|_{T_{h,0}} = B_m' + iB_m''$, $B_h' \equiv d\epsilon_h'/dT|_{T_{h,0}}$ and $B_{\kappa,h} \equiv d\kappa_h/dT|_{T_{h,0}}$. For simplicity, we consider hosts which exhibit negligible absorption ($B_h'' = 0$); however, any nonzero contribution will cause only a quantitative difference.

In all the examples below, we limit ourselves to a maximal temperature rise of $\Delta T \approx 300$ K. In this range, the assumptions detailed above hold (see, e.g., Ref. [26]), and one avoids sintering and melting of the metal [32] as well as damage or phase transitions in many possible hosts, thus justifying the neglect of additional thermodynamical considerations (see, e.g., Refs. [33–35]).

III. TEMPERATURE, PERMITTIVITY, AND ELECTRIC FIELD IN A SMALL METAL NANOSPHERE

With the assumptions above, Eqs. (1) and (2) reduce to a fourth-order polynomial equation in ΔT, namely

$$\underbrace{\frac{B_{\kappa,h}}{\kappa_{h,0}}\frac{B_{\rm tot}'^2 + B_m''^2}{\epsilon_{m,0}''^2}}_{a_4}\Delta T^4 + \underbrace{\left[\frac{B_{\rm tot}'^2 + B_m''^2}{\epsilon_{m,0}''^2} + 2\frac{B_{\kappa,h}}{\kappa_{h,0}}\frac{B_{\rm tot}'\epsilon_{\rm tot}' + B_m''\epsilon_{m,0}''}{\epsilon_{m,0}''^2} - \Delta T_I^{\rm on}\frac{B_h'^2}{\epsilon_{h,0}'^2}\frac{B_m''}{\epsilon_{m,0}''}\right]}_{a_3}\Delta T^3$$

$$+ \underbrace{\left[2\frac{B_{\rm tot}'\epsilon_{\rm tot}' + B_m''\epsilon_{m,0}''}{\epsilon_{m,0}''^2} + \frac{B_{\kappa,h}}{\kappa_{h,0}}\left(1 + \frac{\epsilon_{\rm tot}'^2}{\epsilon_{m,0}''^2}\right) - \Delta T_I^{\rm on}\left(2\frac{B_h'}{\epsilon_{h,0}'}\frac{B_m''}{\epsilon_{m,0}''} + \frac{B_h'^2}{\epsilon_{h,0}'^2}\right)\right]}_{a_2}\Delta T^2$$

$$+ \underbrace{\left[\left(1 + \frac{\epsilon_{\rm tot}'^2}{\epsilon_{m,0}''^2}\right) - \Delta T_I^{\rm on}\left(\frac{B_m''}{\epsilon_{m,0}''} + 2\frac{B_h'}{\epsilon_{h,0}'}\right)\right]}_{a_1}\Delta T = \Delta T_I^{\rm on}, \tag{4}$$

where $B_{\rm tot}' \equiv B_m' + 2B_h'$ and

$$\Delta T_I^{\rm on} \equiv \frac{3\omega\epsilon_0}{2}\frac{a^2}{\kappa_{h,0}}\frac{\epsilon_{h,0}'^2}{\epsilon_{m,0}''}|\vec{E}_{\rm inc}|^2 = \frac{a^2}{\kappa_{h,0}}\frac{3\omega\epsilon_{h,0}'^{3/2}}{4c\epsilon_{m,0}''}I_{\rm inc} > 0 \tag{5}$$

is the temperature rise in the on-resonance case when all thermoderivatives vanish [36], i.e., it is the first-order approximation of Eq. (4), hence, the reason for the subscript I; the superscript *on* is shorthand for "on resonance", see below. Here $I_{\rm inc} = 2\sqrt{\epsilon_{h,0}'}|\vec{E}_{\rm inc}|^2/Z_0$ is the incident intensity. More generally, $\Delta T_I^{\rm on}$ is proportional to $P_{\rm abs}$, the density of power absorbed within the sphere, namely $\Delta T_I^{\rm on} = P_{\rm abs}/4\pi\kappa_{h,0}a$ [21]. This result was referred to in Ref. [19] as the *temperature-independent permittivity model*.

A few points can already be noted. First, the coefficients in Eq. (4) involve only the relative temperature-induced changes of the optical and thermal properties rather than the absolute changes of these quantities. In fact, quite unintuitively, the real part of the thermoderivatives of the metal permittivity turns out to be normalized by the imaginary part of the permittivity rather than by the real part; on the other hand, the (real part of the) thermoderivative of the host permittivity is normalized by the real part of the host permittivity. Second, it is clear that one can distinguish between two generic scenarios: when the illumination is on-resonance ($\epsilon_{\rm tot}' \ll \epsilon_{m,0}''$) or off-resonance (otherwise) . We showed in Ref. [19] that there is a qualitative difference between these two cases, something which can, in fact, be observed from the first-order approximation of Eq. (4) (i.e., when all the thermoderivatives vanish),

$$\Delta T_I = \frac{\epsilon_{m,0}''^2}{\epsilon_{m,0}''^2 + \epsilon_{\rm tot}'^2}\Delta T_I^{\rm on}. \tag{6}$$

Indeed, Eq. (6) shows that in the off-resonance case, the temperature rise is higher for increasing $\epsilon_{m,0}''$, while the opposite is true for the on-resonance case. This is a standard signature of the resonance, affecting the absorption and quality factor of this plasmonic resonator.

Equations (5) and (6) are the basis for the perturbative description of the thermal nonlinearity of metals (as a cubic nonlinearity), where $\chi_m^{(3)}|\vec{E}_m|^2 \sim B_m\Delta T_I$ [13]. Any deviation from this solution, specifically, a more accurate solution

for the temperature rise that accounts for the higher-order coefficients $a_{j>1}$, will give rise to a deviation from the standard perturbative description of a cubic nonlinear response [37]. The resulting thermo-optical nonlinearity will be, in general, nonperturbative (i.e., requiring one to go beyond a model with a cubic (and even a cubic-quintic) nonlinearity), despite the fact that the permittivity is linearly dependent on the temperature [see (3)]. While this may not be a new or surprising observation, we emphasize that, unlike the well-studied ultrafast nonlinearity [23], the CW nonlinearity of metals in general, and of a single metal nanosphere in particular, was not studied systematically at all [19]. Accordingly, in this article, we aim to study this case in detail.

We will do that in two stages. First, we will solve Eq. (4) for a varying level of illumination. Despite its considerable simplicity, the analytical solution of Eq. (4) is too complicated for meaningful physical interpretation. Accordingly, we proceed by a numerical solution of Eq. (4) . We also compare the exact solution of Eq. (4) to its third-order approximation, i.e., the solution of Eq. (4) for $a_4 = 0$, to its second-order approximation (i.e., with $a_3 = a_4 = 0$), as well as to its first-order approximation ($a_2 = a_3 = a_4 = 0$), i.e., Eq. (6) [38].

We will then use the expressions for the temperature rise to study the dependence of the permittivity (3) and field (2) on the incoming intensity. When referring to these quantities, we loosely adopt below the standard terminology of nonlinear optics, namely the term proportional to $I_{\rm inc} \sim |E_{\rm inc}|^2$ will be referred to as the cubic nonlinear term and the term proportional to $I_{\rm inc}^2 \sim |E_{\rm inc}|^4$ will be referred to as the quintic nonlinear term, etc. (although the proper nonlinear coefficients should be defined with respect to the local field rather than the incident one).

IV. NUMERICAL EXAMPLES

Below, we describe several configurations based on noble metals and generic dielectric hosts. Additional materials can be analyzed along the same lines [39]. We focus on the optical regime in order to be in the spectral vicinity of the plasmon resonances of small nanospheres and since the infrared regime is not so interesting in the context of nonlinear optical response due to the lack of intense sources (see discussion in Ref. [19]).
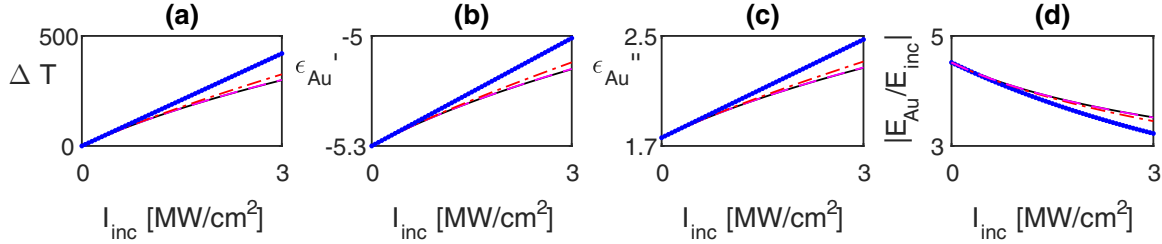
FIG. 1. (a) The temperature rise (4) inside a Au nanosphere ($a = 10$ nm) in an oil host ($\epsilon_h = 2.65$) illuminated at $\lambda = 550$ nm as a function of the incident intensity (black solid line); see values of additional parameters in the main text. The solutions accounting for up to third, second, and first-order terms are shown by magenta dashed, red dash-dotted, and blue dotted lines, respectively; however, the black and magenta lines are essentially indistinguishable. (b) Real and (c) imaginary parts of the Au permittivity (3) as a function of the incoming intensity, based on the various solutions for ΔT shown in (a). (d) Same as in (b) and (c) for the normalized electric field (2) within the Au nanosphere.

Finally, without loss of generality, we choose $a = 10$ nm to avoid quantum size effects [40]. Equation (5) shows that under the quasistatic approximation used here, a change of the nanosphere radius is equivalent to a rescaling of the incident intensity; for smaller nanospheres, it would be necessary to account for modification of ϵ_m due to quantum size corrections.

The quantitative discussion below will refer to the values obtained at the maximal incoming intensity.

A. Au nanospheres in a liquid host

We set $\lambda = 550$ nm such that $\epsilon_{Au,0} = -5.3 + 1.76i$ and $B_{Au} = (0.7 + 1.7i) \cdot 10^{-3}/\deg$ K [27]; thus, $B_{Au}/\epsilon''_{Au,0} \sim (0.4 + i) \times 10^{-3}/\deg$ K and for $\epsilon'_{h,0} = 2.65$, the illumination is resonant. We also set $B'_h = 10^{-4}/\deg$ K [41] (so $B'_h/\epsilon'_{h,0} \sim 3 \times 10^{-5}/\deg$ K) and $\kappa_{h,0} = 0.15$ W/m/deg K; all these parameters correspond to an index matching oil, as used in the experiments of Refs. [8–12]. In the absence of concrete data, we estimate $B_{\kappa,h} = 5 \times 10^{-5}$ W/m/deg K^2 such that $B_{\kappa,h}/\kappa_{h,0} \sim 3 \times 10^{-4}/\deg$ K, and at $\Delta T = 300$ K, and the change of κ_h is $\sim 10\%$.

Figure 1(a) shows the solution of Eq. (4). One can see that the temperature grows monotonically with the incoming intensity but with a decreasing slope; this behavior is reminiscent of saturation, but in the current case the temperature does not have an asymptotic value. The deviation of the solution of the fourth-order polynomial (4) from its first-order approximation (5) reaches several tens of percent (as seen before in Ref. [19]). However, this deviation decreases to less than 10% and even less than 0.5% when the second-order and third-order terms, respectively, are accounted for.

Figures 1(b) and 1(c) show the corresponding changes of the real and imaginary parts of the Au permittivity, respectively. The relative change of ϵ'_{Au} is a few percent, but the relative increase of ϵ''_{Au} reaches $\sim 30\%$; As noted, this is an unusually high nonlinearity, especially in light of the short propagation distance with which it is associated. Importantly, this behavior is opposite to what is known as saturable absorption. In the latter, the permittivity drops and the field increases (locally), while in our case, the opposite happens [42]. Figures 1(b) and 1(c) also show approximations of the exact solution of Eq. (4), based on either the second-order and third-order approximations, respectively. As seen, *the first-order approximation provides a good match to the exact results only up to a temperature rise of about 100* K, beyond

which the standard perturbative (cubic) description of the metal nonlinearity is inadequate. Instead, the second-order approximation provides a decent match to the exact solution within the current temperature range, reflecting the slowing down ("saturation") of the temperature rise. The permittivity based on the third- and fourth-order approximations for the temperature rise are naturally indistinguishable. This shows that *although the nonlinearity is extremely strong, it is weaker than what the first-order, standard perturbative (cubic) solution predicts, due to the slowing down of the temperature rise*.

Finally, Fig. 1(d) shows the field within the nanosphere. As expected, it decreases due to the increase of ϵ''_m, see Eq. (2), which in turn, causes the slower rise of the temperature. Again, while the first-order approximation is accurate only for a limited range of temperatures (hence, intensities), the second-order approximation is in reasonable agreement with the exact numerical results while the third-order approximation is, again, essentially indistinguishable from the exact solution. As shown in Ref. [19], the scattered field follows the same trend.

One can verify the that other thermoderivatives have indeed a lesser impact on the temperature rise and field. Indeed, a direct test of the importance of B'_m shows that setting its value to zero leads to a maximal error smaller than 1% (~ 3 K) in the temperature rise (with respect to a $\sim 100\%$ total temperature rise of ~ 300 K); the relative errors in the permittivity and field are of comparable magnitude. A similar error is incurred by setting $B'_h = 0$. In comparison, setting $B_{\kappa,h} = 0$ leads to a relative error of $\sim 7\%$ for the temperature rise [43]. These changes are in good agreement with the analysis, see Sec. V.

B. Au nanospheres in a AlGaAs host

We now choose a solid host, specifically Al$_x$Ga$_{1-x}$As with $x = 30\%$ Al content, such that the host is transparent throughout the infrared spectral range and exhibits a rather high permittivity of ~ 13 near the band edge (i.e., about 5 times higher than the oil liquid employed above). Accordingly, the localized plasmon resonance occurs at $\lambda = 800$ nm, where $\epsilon_{Au,0} = -26.5 + 2i$ [26]; in addition, $B_{Au} = (2 + 2.6i) \times 10^{-3}/\deg$ K so $B_{Au}/\epsilon''_{Au,0} = (1 + 1.3i) \times 10^{-3}/\deg$ K; this choice corresponds to the largest value of $B''_{Au}/\epsilon''_{Au,0}$ in the optical spectral domain.

This choice of Al content also corresponds to nearly minimal value of thermal conductivity, $\kappa_{h,0} \approx 13$ W/m/deg K [44], which is about 100 times higher than for the previous
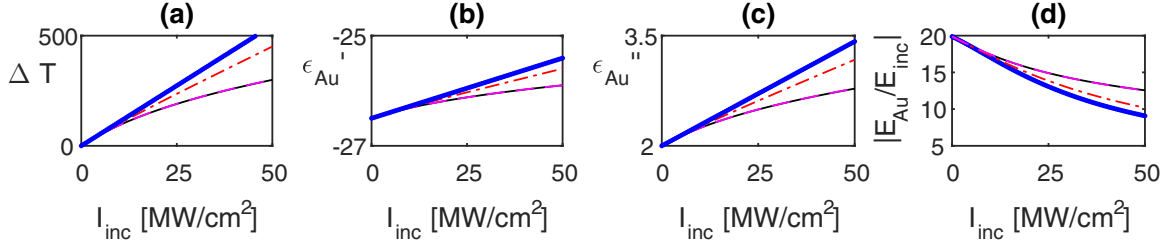
FIG. 2. Same as Fig. 1 for a $Al_{0.3}Ga_{0.7}As$ host with $\lambda = 800$ nm and $\epsilon'_{h,0} = 13$.

example (oil) but still about 20 times smaller than for metals. Thus, the error associated with neglecting the temperature nonuniformity amounts to no more than 2% [19]. This error is much smaller than all the effects demonstrated below.

Based on data for GaAs [45], we estimate $B'_{\text{AlGaAs}} \approx 2 \times 10^{-3}/\text{deg K}$ (such that $B'_{\text{AlGaAs}}/\epsilon''_{\text{AlGaAs},0} \sim 10^{-3}/\text{deg K}$; this is an order of magnitude higher than in the previous example) and estimate $B_{\kappa,h} = 5 \times 10^{-4}$ W/m/deg K^2 such that at $\Delta T = 300$ K, the change of κ_h is $\sim 1\%$, i.e., it is negligible. We ignore strain or stress that may develop within the solid host due to the heating. These effects may only increase the nonlinear response.

The results shown in Fig. 2 are qualitatively similar to the case of a liquid host (Fig. 1), however, for ΔT_l^{on} which is ~ 13 times smaller [46]. This is a direct result of the heat diffusion in the host and, more generally, of the spatially nonlocal nature of the thermal nonlinearity in the system, causing lower effective heating of the metal nanosphere. This also shows, in contrast to what one may expect based on the near-field enhancement [see Eqs. (13)–(15) below] and the ultrafast case (see, e.g., Refs. [47,48] and discussion below), that the metal-semiconductor system is *less* nonlinear than the metal-liquid system for CW illumination.

Another difference between Figs. 1 and 2 is that in the latter, the second-order approximation of Eq. (4) provides a poorer match to the exact variations of the permittivity and field compared to the previous example. This can be traced to the relatively larger value of the (relative) change of the host permittivity, which makes the third-order term in Eq. (4) dominant.
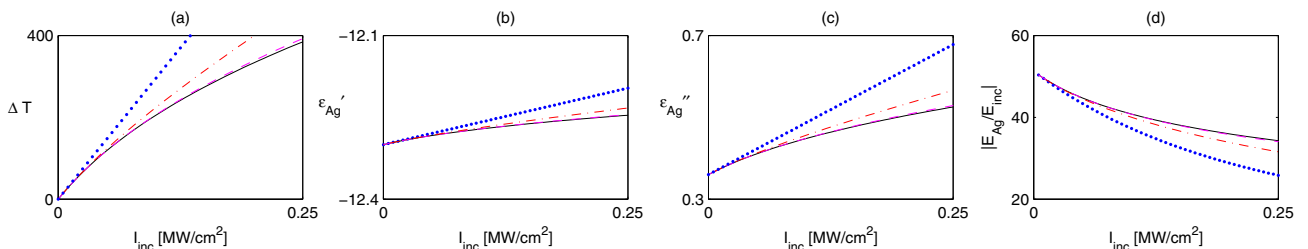
C. Ag nanospheres

We now replace the Au sphere with a Ag sphere. For $\lambda = 550$ nm, it follows from Ref. [24] that $\epsilon_{Ag,0} = -12.3 + 0.36i$ and $B_{Ag} = (14 + 43i) \times 10^{-5}/\text{deg K}$ such that $B_{Ag}/\epsilon''_{Ag,0} \sim 10^{-3}i$ and the illumination is resonant for $\epsilon'_{h,0} = 6.15$. The most striking difference between the results shown in Fig. 3

with respect to previous examples is the stronger nonlinearity. Indeed, ΔT reaches ≈ 300 K at much lower intensities, a direct result of the much lower imaginary part of the Ag permittivity, which gives rise to a more efficient absorption. Apart from that, the results are qualitatively similar to those shown above. Again, the properties of the dielectric host prove to be of lesser importance. Thus, the relative nonlinearities of Au and Ag for CW illumination are different from those reported for femtosecond illumination [49].

In Fig. 4, we present results based on the alternative data source for Ag given in Ref. [50]. For example, for the same wavelength, Ref. [50] gives $\epsilon_{Ag,0} = -8.5 + 1.8i$ and $B_{Ag} = (-6.2 + 1.2i) \times 10^{-3}/\text{deg K}$ such that $B_{Ag}/\epsilon''_{Ag,0} \sim (-3.4 + 0.66i) \times 10^{-3}$ and the illumination is resonant for $\epsilon'_{h,0} \sim 4$. The large differences between the permittivities and thermoderivatives in these data sets can be traced to the lower quality of the Ag film from which the permittivity data was extracted compared with Ref. [24]; beyond the well-studied changes of the permittivity itself, this can give rise to modifications of the metal volume morphology during the measurements themselves and, hence, to overall larger thermoderivatives, see corresponding discussion in Refs. [26,27,51]. Yet, this data set is still worth studying because the morphology of the nanoparticle is rarely perfect and depends sensitively on the details of the synthesis.

Due to the higher value of $\epsilon''_{m,0}$ compared to Ref. [24], the nonlinear response is smaller than that shown in Fig. 3 and similar to that shown for Au (Figs. 1 and 2). A direct test of the relative importance of B'_m and B''_m shows that the importance of $B'_m(/\epsilon''_{m,0})$ is comparable to that of $B''_m(/\epsilon''_{m,0})$ although the latter is about 6 times smaller. This is in agreement with the analysis shown below.

We also note that the data of Ref. [50] suggests an even more extreme case where $B'_m \gg B''_m$ (occurring at $\lambda \approx 450$ nm) [52]. Only then does B'_m dominate the changes of the temperature and field. Such a case could open up additional possibilities, such as increasing the scattering by shifting into resonance, see Ref. [[53], Sec. IV C].

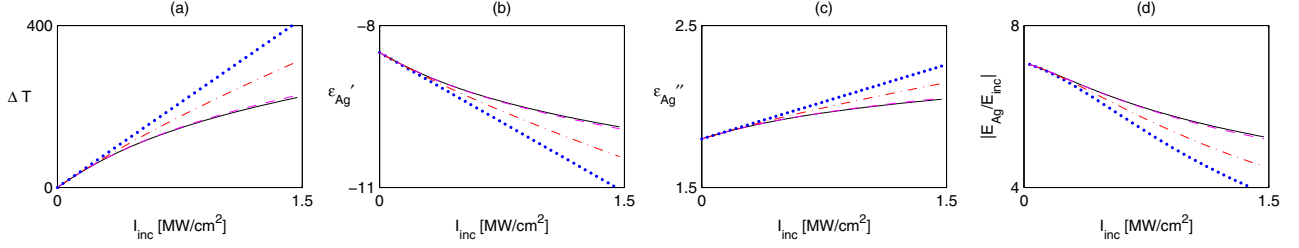FIG. 3. Same as Fig. 1 for a Ag nanosphere (permittivity data taken from Ref. [24]) and $\epsilon'_{h,0} = 6.15$.

FIG. 4. Same as Fig. 3 but with the permittivity data taken from Ref. [50], hence, with $\epsilon'_{h,0} \sim 4$.

V. FURTHER ANALYSIS AND SIMPLIFICATION

A. A second-order approximation of the temperature rise

We saw that the third-order approximation of the temperature rise (4) is essentially indistinguishable from the exact solution. However, as for the analytical form of the exact solution, it is hard to extract physical insights from the analytical form of the third-order approximation either is reasonably accurate in most cases shown above. We would now like to use it in order to further elucidate the relative importance of the various physical effects and how each of them affects the temperature [54].

The solution of Eq. (4) for $a_3 = a_4 = 0$ is

$$\Delta T = \frac{a_1}{2a_2}\left(\sqrt{1 + 4\frac{a_2}{a_1^2}\Delta T_I^{\text{on}}} - 1\right). \quad (7)$$

This shows that in general, the temperature rise does not scale linearly with the incoming intensity [via ΔT_I (6)] as one would expect from the standard perturbative (cubic) description of the thermo-optical nonlinearity; instead, it follows a square-root law, i.e., it grows more slowly (for $a_2 > 0$, which is the usual case [55]); this behavior was referred to as above as a slowdown of the temperature rise.

We can expand the square root in Eq. (7) in a Taylor series such that

$$\Delta T = \frac{\Delta T_I^{\text{on}}}{a_1} - \frac{a_2}{a_1^3}\left(\Delta T_I^{\text{on}}\right)^2 + \cdots, \quad (8)$$

where ΔT_I^{on} (5) scales with I_{inc}, a^2, and $\kappa_{h,0}^{-1}$; similarly, the nonlinear correction to the temperature scales with I_{inc}^2, a^4, and $\kappa_{h,0}^{-2}$.

We note that some of the contributions to the coefficients a_1 to a_3 are proportional to ΔT_I^{on}. These will, naturally, contribute only to the next order in ΔT_I^{on} (or, equivalently, in I_{inc}). Specifically, this shows that although B''_m and B'_h appear in a_1, they affect the temperature rise ΔT only via the quintic (and higher) nonlinearity, as does $B_{\kappa,h}$.

Further distinction between the various contributions can be attained by noting that, *typically*, the permittivity of a (host) *dielectric* material is less sensitive to temperature than a metal, i.e.,

$$B'_h/\epsilon'_{h,0} \ll |B_m|/\epsilon''_{m,0}. \quad (9)$$

Indeed, one can compare, e.g., recent ellipsometry results [24,26,27,50] with values detailed in Ref. [1]; see also specific examples above . However, one cannot say anything in general about the relative magnitude of $\kappa_{h,0}/B_{\kappa,h}$.

Even further distinction can be made for a specific spectral configuration. At resonance, i.e., for $\epsilon''_{m,0} \gg \epsilon'_{\text{tot}} \to 0$, Eq. (4) reduces to

$$\underbrace{\left[2\frac{B''_m}{\epsilon''_{m,0}} + \frac{B_{\kappa,h}}{\kappa_{h,0}} - \Delta T_I^{\text{on}}\left(2\frac{B''_m B'_h}{\epsilon''_{m,0}\epsilon'_{h,0}} + \frac{B'^2_h}{\epsilon'^2_{h,0}}\right)\right]}_{a_2}\Delta T^2$$
$$+ \underbrace{\left[1 - \Delta T_I^{\text{on}}\left(\frac{B''_m}{\epsilon''_{m,0}} + 2\frac{B'_h}{\epsilon'_{h,0}}\right)\right]}_{a_1}\Delta T = \Delta T_I^{\text{on}}. \quad (10)$$

Organizing the orders of ΔT_I^{on}, Eq. (8) reduces to

$$\Delta T = \Delta T_I^{\text{on}} - \left(\frac{B''_m}{\epsilon''_{m,0}} + \frac{B_{\kappa,h}}{\kappa_{h,0}} + 2\frac{B'_h}{\epsilon'_{h,0}}\right)\left(\Delta T_I^{\text{on}}\right)^2 + \cdots. \quad (11)$$

Note that the various thermoderivatives may not necessarily have the same sign so they can balance each other. However, as noted [see Eq. (9)], $B'_h/\epsilon'_{h,0}$ is typically smaller with respect to $B''_m/\epsilon''_{m,0}$, so its sign is of lesser importance and the coefficient of the quintic nonlinearity can be simplified. In addition, Eqs. (10) and (11) show that in this case, B'_m appears only beyond the quintic order. This explains the relative importance of B''_m and $B_{\kappa,h}$ for the temperature rise in the examples above.

Away from resonance, i.e., for $\epsilon'_{\text{tot}} \gg \epsilon''_{m,0}$, Eq. (8) can be approximated by

$$\Delta T \approx \left(\frac{\epsilon''_{m,0}}{\epsilon'_{\text{tot}}}\right)^2 \Delta T_I^{\text{on}} - \left\{\frac{B''_m}{\epsilon''_{m,0}} + 2\frac{B'_h}{\epsilon'_{h,0}}\right.$$
$$+ \left[2\frac{B'_{\text{tot}}\epsilon'_{\text{tot}}}{\epsilon''^2_{m,0}} + \frac{B_{\kappa,h}}{\kappa_{h,0}}\left(\frac{\epsilon''_{m,0}}{\epsilon'_{\text{tot}}}\right)^{-2}\right]\left(\frac{\epsilon''_{m,0}}{\epsilon'_{\text{tot}}}\right)^6 \left.\right\}\left(\Delta T_I^{\text{on}}\right)^2$$
$$+ \cdots. \quad (12)$$

Thus, with respect to the on-resonance case, the cubic term is smaller and the weights of the various thermoderivatives differ for the quintic coefficient. Specifically, the quintic term now includes also B'_m.

B. The effects of the thermoderivatives on the electric field

From the linear dependence of the permittivities on the temperature (see Sec. II), it follows that the field within the nanosphere is

$$\vec{E}_m[\Delta T(\vec{E}_{\text{inc}})] = \left(\frac{1 + \frac{B'_h}{\epsilon'_{h,0}}\Delta T}{1 + \frac{B'_{\text{tot}} + iB''_m}{\epsilon'_{\text{tot}} + i\epsilon''_{m,0}}\Delta T}\right)f_0\vec{E}_{\text{inc}}, \quad (13)$$

where

$$f_0 \equiv 3\epsilon'_{h,0}/(\epsilon'_{\text{tot}} + i\epsilon''_{m,0}), \qquad (14)$$

is the usual figure of merit for field enhancement inside a nanosphere [13,47], sometimes referred to as the Faraday number [48]. This shows that the dependence of the field within the nanosphere on the temperature rise is not linear.

At resonance, this reduces to

$$\vec{E}_m[\Delta T(E_{\text{inc}})] = \frac{1 + \frac{B'_h}{\epsilon'_{h,0}}\Delta T}{1 + \left(\frac{B''_m}{\epsilon''_{m,0}} - i\frac{B'_{\text{tot}}}{\epsilon''_{m,0}}\right)\Delta T} f_0^{(\text{res})} \vec{E}_{\text{inc}}, \qquad (15)$$

where $f_0^{(\text{res})} \equiv -3i\epsilon'_{h,0}/\epsilon''_{m,0}$. Thus, although the thermoderivatives of the permittivities affect the temperature only at second order, they do affect the field on first order [56]. Specifically, $B''_m > 0$ leads to a weaker field [via a decrease of the field enhancement (hence, Q factor)]. In contrast, $B'_h > 0$ leads to an increase of the field, *although* it causes also a shift away from resonance. Indeed, a Taylor expansion of the denominator of Eq. (15) shows, somewhat unintuitively, that $|B'_{\text{tot}}|$, hence, the shift away from resonance and specifically, $|B'_m|$, affect the electric field only at order ΔT^2 (naturally, it causes a decrease of the field inside the nanosphere). This is a generic result, i.e., it applies to all metals, regardless of the relative importance of intraband and interband transitions or the spectral width of the resonance. As noted, the spectral shift from resonance becomes important only when $B'_m \gg B''_m$, see Sec. IV C. This result is also independent of the accuracy of the calculation of the temperature (i.e., it is more accurate than the approximations described in Sec. V A). In fact, this analysis applies for any intensity-dependent nonlinearity, i.e., it is not limited to permittivity changes associated with a temperature rise these theoretical results are in excellent agreement with the pump-probe experiments reported in [12] where the linewidth increased by ∼16% but the resonance shift was negligible.

Away from resonance B'_m has a comparable effect to that of the other thermoderivatives.

VI. DISCUSSION AND OUTLOOK

The numerical examples and consequent approximate analysis above show that the nonlinear thermal response is extremely strong, especially considering the short propagation distances involved; however, it is cubic in nature only for a modest temperature rise of up to about 100 K; this is a regime where the nonlinear response is, in fact, frequently ignored altogether. We show that beyond this regime, the growth of the temperature and nonlinearity slows down, such that a nonperturbative description of the nonlinear response is needed. Remarkably, unlike many other materials for which such "saturation"-like behavior occurs at relatively weak nonlinearities, in the current context, this happens when the permittivity changes already by several tens of percent. Thus, this sphere problem offers a nonperturbative nonlinearity with no need for a nearly vanishing permittivity, as in Refs. [5–7].

Overall, we saw that the changes of the metal permittivity dominate the nonlinear thermal response of the nanosphere configuration. However, this does not mean that the effects of thermal lensing (in particular, distortion of the incoming field due to inhomogeneous heating of the host) are secondary.

Indeed, the host occupies a much larger fraction of space (unless the nanoparticles are at a high density). Thus, the relative importance of heating the metal and host should be studied using effective medium techniques; a first step towards this goal was already described in Refs. [57,58]. A more detailed study should appear in a separate paper.

It is tempting to write the temperature-dependent term in Eq. (3) as the product of the intensity and the cubic nonlinear coefficient associated with the thermal effect and similarly for the quintic nonlinear coefficient, etc. However, strictly speaking, such an expansion (3) *cannot* be regarded as an inherent material parameter, because although the expression for the temperature rise involves the intrinsic material electromagnetic response of the metal, it also involves, as would happen for any structure, the size of the nanosphere, and the electromagnetic and thermal response of the host [59]. Thus, specifically, the values of the nonlinear coefficients reported in Ref. [12] cannot be compared to other reported values of the intrinsic nonlinearity of metals. On the other hand, the temperature-dependent term (3) cannot be understood as an effective nonlinearity of a composite either, since such a quantity necessarily involves the fill factor, interparticle interactions, etc., none of which were considered in our calculations of the temperature rise.

Thus, the correction to the permittivity, $B_m\Delta T$, or its leading-order approximation, $B_m\Delta T_I$, should be understood as a figure of merit (FOM) for the nonlinear response. Note that our FOM, $B_m\Delta T_{(I)}$, is proportional to the absorption cross section of the nanosphere or, equivalently, to the Joule number [48]. It, however, includes also information about the absolute temperature rise for a given incoming intensity and host by accounting for heat diffusion in the host. Specifically, our FOM reflects the competition between a high permittivity host, which yields a higher field enhancement and, hence, stronger nonlinear response on resonance, but may also entail a high thermal nonlinearity which will cause the opposite effect. Accordingly, while the conventional FOM (Eq. (14) and [47,48]) is relevant globally for linear optics, in the context of intense illumination, it is useful only for ultrafast nonlinearities where the thermal properties do not play an important role, i.e., when the nonlinear response is spatially local. However, for the many applications associated with intense CW illumination (see discussion in Ref. [19]), our FOM should be used.

The qualitative match of our results to experimental results of nonlinear scattering of CW light from the small nanospheres [19] supports their interpretation as a thermal nonlinear effect. However, many effects, some of which do not play an important role in the ultrafast case, may have a non-negligible contribution in the CW case and, hence, may affect the quantitative match the between numerical and experimental results; these include specifically, stress or strain within a solid host and/or acoustic oscillations in a liquid (see, e.g., Ref. [60]) or purely electronic effects such as partial population inversion due to interband transitions [13] and associated free-carrier generation, multiphoton absorption, etc. We are not aware of any previous systematic comparative study of the various contributions to the CW nonlinearity in the single-particle case [61]. The suggestions detailed below can provide a first step towards such a goal.

The most direct way to do that would be to measure the temperature in the near-field. Although such measurements

are quite challenging, there is growing interest in developing such techniques [62–67]. These can validate the calculations above even without nanometric resolution.

A simpler alternative would be to measure the far-field scattering of the electromagnetic waves for hosts with different levels of thermal conductivities. This property is unique to the thermal response and, hence, will give direct evidence regarding the role of the thermal effect. An attempt to do that was made in Ref. [68]. However, like most previous studies, Ref. [68] involved a suspension of particles rather than a single particle. It also compared composites with different densities (details not provided), which may involve different effective response due to the long-range nature of the thermal interactions between adjacent nanospheres. Worse than that, this study ignored various additional relevant factors like the size of the particles that affects the leading order approximation ΔT_I (6). It also ignored the Kapitza resistance and its temperature and size dependence.

These inconsistencies can explain the large discrepancies in Ref. [68] between the simplistic theoretical prediction (based solely on the value of the thermal conductivity) and the experimental observations. A more accurate match requires accounting for all the additional parameters and for potential absorption in the host. Obviously, if the signal is collected from more than a single particle, then one has to compare the measurement to a full effective medium theory for a composite with a strong nonlocal nonlinearity. Such a theory does not currently exist to the best of our knowledge. Once all these issues are accounted for, it would be possible to ascribe any remaining differences with nonlinear effects that do not involve heating.

The results shown above were for nanospheres of a total size of 20 nm. For smaller nanospheres, the results scale with intensity [as per Eq. (6)], with the additional possibility of increased absorption due to quantum size effects. On the opposite limit, for larger particles, one may have to account for the growing nonuniformity of the field and temperature. Following the linear calculation in Ref. [22], we believe that all the claims above would apply also to such larger spheres, as well as to particles of other shapes, with only quantitative differences.

Our results were also limited to a modest temperature rise of ≈ 300 K. Beyond that range, the thermoderivatives are not necessarily constant, giving rise to further deviation from the perturbative description. In addition, other effects (which we believe are weaker at moderately high incident intensities) may become important for higher temperatures or intensities, e.g., multiphoton absorption, and nonthermal effects. In the presence of the latter, one may not be able to use the high-temperature ellipsometry results of Refs. [24,26,27,50] which

are strictly relevant only for metals at thermal equilibrium, i.e., metals whose electrons obey the Fermi-Dirac distribution. In the context of pulsed illumination, these effects are frequently linked to saturable absorption (= partial population inversion) due to interband transitions, see Ref. [13] and later studies, e.g., Refs [16–18]. Indeed, such effects may explain the small increase of scattering observed in some of these studies. However, to the best of our knowledge, no conclusive proof regarding the origin of the increased scattering was ever given, nor any quantitative prediction. For CW, a much more significant increase of scattering was observed in Refs. [8–11]; however, similarly, its origin is still not understood. The current study shows that the likelihood of this scattering increase to be related with changes of the host are low, but it does not rule them out completely. Clearly, at even higher temperatures, the metal would undergo sintering and eventually melting, and the host may undergo a phase transition or get damaged; in these cases, additional thermodynamic considerations may apply (see, e.g., Refs. [33–35,69,70]).

Beyond the context of the thermo-optical nonlinearity, the approach described in this article can be employed to improve the modeling of particle size reduction [33,34], bubble formation [35,69,70], photothermal imaging [71,72], and photoacoustic imaging [60,73,74].

As a final statement, this study provides an important step towards the characterization of the effective response of arrays of particles, which can be regarded as thermo-optical metamaterials—artificial materials that change their electromagnetic properties under laser illumination due to temperature rise. These would have to be studied under proper effective medium theory and beyond the perturbative description, accounting not only for the electromagnetic interactions between the nanoparticles but also for the thermal interactions between them. The latter is expected to have a far longer length scale. This fact, together with the use of an absorptive nonlinearity, may allow us to surpass the limitations detailed in Ref. [4] for highly nonlinear metamaterials.

[1] R. W. Boyd, *Nonlinear Optics*, 2nd ed. (Academic Press, San Diego, CA, 2003).

[2] G. P. Agrawal, *Nonlinear Fiber Optics*, 3rd ed. (Academic Press, San Diego, CA, 2001).

[3] Q. Lin, O. J. Painter, and G. P. Agrawal, Nonlinear optical phenomena in silicon waveguides: modeling and applications, Opt. Express **15**, 16604 (2007).

[4] J. B. Khurgin and G. Sun, Plasmonic enhancement of the third order nonlinear optical phenomena: Figures of merit, Opt. Express **21**, 27460 (2013).

[5] L. Caspani, R. P. M. Kaipurath, M. Clerici, M. Ferrera, T. Roger, J. Kim, N. Kinsey, M. Pietrzyk, A. Di Falco, V. M. Shalaev, A. Boltasseva, and D. Faccio, Enhanced Nonlinear Refractive Index in ϵ-Near-Zero Materials, Phys. Rev. Lett. **116**, 233901 (2016).

[6] M. Z. Alam, I. De Leon, and R. W. Boyd, Large optical nonlinearity of indium tin oxide in its epsilon-near-zero region, Science **352**, 795 (2016).

[7] O. Reshef, E. Giese, M. Z. Alam, I. De Leon, J. Upham, and R. W. Boyd, Beyond the perturbative description of the nonlinear optical response of low-index materials, arXiv:1702.04338.

[8] S.-W. Chu, H.-Y. Wu, Y.-T. Huang, T.-Y. Su, H. Lee, Y. Yonemaru, M. Yamanaka, R. Oketani, S. Kawata, and K. Fujita, Saturation and reverse saturation of scattering in a single plasmonic nanoparticle, ACS Photon. **1**, 32 (2013).

[9] S.-W. Chu, T.-Y. Su, R. Oketani, Y.-T. Huang, H.-Y. Wu, Y. Yonemaru, M. Yamanaka, H. Lee, G.-Y. Zhuo, M.-Y. Lee, S. Kawata, and K. Fujita, Measurement of a Saturated Emission of Optical Radiation from Gold Nanoparticles: Application to an Ultrahigh Resolution Microscope, Phys. Rev. Lett. **112**, 017402 (2014).

[10] H. Lee, R. Oketani, Y.-T. Huang, K.-Y. Li, Y. Yonemaru, M. Yamanaka, S. Kawata, K. Fujita, and S.-W. Chu, Point spread function analysis with saturable and reverse saturable scattering, Opt. Express **22**, 26016 (2014).

[11] Y.-T. Chen, P.-H. Lee, P.-T. Shen, J. Launer, R. Oketani, K.-Y. Li, Y.-T. Huang, S. Shoji, S. Kawata, K. Fujita, and S.-W. Chu, Study of nonlinear plasmonic scattering in metallic nanoparticles, ACS Photon. **3**, 1432 (2016).

[12] H.-Y. Wu, Y.-T. Huang, P.-T. Shen, H. Lee, R. Oketani, Y. Yonemaru, M. Yamanaka, S. Shoji, K.-H. Lin, C.-W. Chang, S. Kawata, K. Fujita, and S.-W. Chu, Ultrasmall all-optical plasmonic switch and its application to superresolution imaging, Sci. Rep. **6**, 24293 (2016).

[13] F. Hache, D. Ricard, C. Flytzanis, and U. Kreibig, The optical Kerr effect in small metal particles and metal colloids: The case of gold, Appl. Phys. A **47**, 347 (1988).

[14] D. D. Smith, G. Fischer, R. W. Boyd, and D. A. Gregory, Cancellation of photoinduced absorption in metal nanoparticle composites through a counterintuitive consequence of local field effects, J. Opt. Soc. Am. B **14**, 1625 (1997).

[15] D. D. Smith, Y. Yoon, R. W. Boyd, J. K. Campbell, L. A. Baker, R. M. Crooks, and M. George, Z-scan measurement of the nonlinear absorption of a thin gold film, J. Appl. Phys. **86**, 6200 (1999).

[16] U. Gurudas, E. Brooks, D. M. Bubb, S. Heiroth, T. Lippert, and A. Wokaun, Saturable and reverse saturable absorption in silver nanodots at 532 nm using picosecond laser pulses, J. Appl. Phys. **104**, 073107 (2008).

[17] H. I. Elim, J. Yang, J.-Y. Lee, J. Mi, and W. Ji, Observation of saturable and reverse-saturable absorption at longitudinal surface plasmon resonance in gold nanorods, Appl. Phys. Lett. **88**, 083107 (2006).

[18] S. Dengler, C. Kübel, A. Schwenke, G. Ritt, and B. Eberle, Near- and off-resonant optical limiting properties of gold-silver alloy nanoparticles for intense nanosecond laser pulses, J. Opt. **14**, 075203 (2012).

[19] Y. Sivan and S.-W. Chu, Nonlinear plasmonics at high temperatures, Nanophotonics **6**, 317 (2017).

[20] In this case, there is only a weak dependence on the spatial shape of the incident field, at least for diffraction-limited far-field illumination.

[21] G. Baffou and R. Quidant, Thermo-plasmonics: Using metallic nanostructures as nano-sources of heat, Laser Photon. Rev. **7**, 171 (2013).

[22] G. Baffou, R. Quidant, and F. J. Garcia de Abajo, Nanoscale control of optical heating in complex plasmonic systems, ACS Nano **4**, 709 (2010).

[23] T. Stoll, P. Maioli, A. Crut, N. Del Fatti, and F. Vallée, Advances in femto-nano-optics: Ultrafast nonlinearity of metal nanoparticles, Eur. Phys. J. B **87**, 260 (2014).

[24] D. T. Owens, C. Fuentes-Hernandez, J. M. Hales, J. W. Perry, and B. Kippelen, A comprehensive analysis of the contributions to the nonlinear optical properties of thin ag films, J. Appl. Phys. **107**, 123114 (2010).

[25] M. Guerrisi, R. Rosei, and P. Winsemius, Splitting of the interband absorption edge in Au, Phys. Rev. B **12**, 557 (1975).

[26] H. Reddy, U. Guler, A. V. Kildishev, A. Boltasseva, and V. M. Shalaev, Temperature-dependent optical properties of gold thin films, Opt. Mater. Express **6**, 2776 (2016).

[27] P.-T. Shen, Y. Sivan, C.-W. Lin, H.-L. Liu, C.-W. Chang, and S.-W. Chu, Temperature- and -roughness dependent permittivity of annealed/unannealed gold films, Opt. Express **24**, 19254 (2016).

[28] R. B. Wilson, B. A. Apgar, L. W. Martin, and D. G. Cahill, Thermoreflectance of metal transducers for optical pump-probe studies of thermal properties, Opt. Express **20**, 28829 (2012).

[29] This is done by assuming that for CW illumination, $T_e = T_l = T$, which is a reasonably good assumption.

[30] H. Reddy, U. Guler, K. Chaudhuri, A. Dutta, A. V. Kildishev, V. M. Shalaev, and A. Boltasseva, Temperature-dependent optical properties of single crystalline and polycrystalline silver thin films, ACS Photon. **4**, 1083 (2017).

[31] G. Baffou and H. Rigneault, Femtosecond-pulsed optical heating of gold nanoparticles, Phys. Rev. B **84**, 035415 (2011).

[32] X. Chen, A. Munjiza, K. Zhang, and D. Wen, Molecular dynamics simulation of heat transfer from a gold nanoparticle to a water pool, J. Phys. Chem. C **118**, 1285 (2014).

[33] L. Hou, M. Yorulmaz, N. R. Verhart, and M. Orrit, Explosive formation and dynamics of vapor nanobubbles around a continuously heated gold nanosphere, New J. Phys. **17**, 013050 (2015).

[34] K. Setoura, Y. Okada, and S. Hashimoto, CW-laser-induced morphological changes of a single gold nanoparticle on glass: observation of surface evaporation, Phys. Chem. Chem. Phys. **14**, 26938 (2014).

[35] G. Baffou, J. Polleux, H. Rigneault, and S. Monneret, Super-heating and micro-bubble generation around plasmonic nanoparticles under CW illumination, J. Phys. Chem. C **118**, 4890 (2014).

[36] Note that ΔT_l^{on} scales with a^2 because it is the ratio of the absorption within the volume, $\sigma_{abs} \sim a^3$, and the rate of heat transfer to the host, given by the product of $\kappa_{h,0}/a$ and the surface area a^2 through which heat diffuses to the host.

[37] This will also happen for a deviation from the linear dependence of the coefficients on the parameters, see Sec. II; however, as explained there, such an effect is not expected within the regime of temperature rise considered in the current study.

[38] In this regard, we note that there are several additional ways to simplify Eq. (4) (see discussion in Sec. V); however, as shown below, none of them is more accurate. Therefore, we choose the simplest way (i.e., setting the $a_{j>1}$ coefficients to zero).

[39] Note that we avoid water as a host in order to avoid complications associated with the limited range of temperature increase before boiling, super heating, and bubble formation [35,69,70].

[40] V. Giannini, A. I. Fernández-Domínguez, S. C. Heck, and S. A. Maier, Plasmonic nanoantennas: fundamentals and their use in controlling the radiative properties of nanoemitters, Chem. Rev. **111**, 3888 (2011).

[41] X. C. Li, J. M. Zhao, L. H. Liu, and J. Y. Tan, Optical properties of edible oils within spectral range from 300 to 2500 nm determined

by double optical pathlength transmission method, Appl. Opt. **54**, 3886 (2015).

[42] In this respect, the original reference to this behavior as saturable scattering [8,9] is highly confusing.

[43] i.e., a temperature increase of 323 deg K instead of 300 deg K. The corresponding errors in the permittivity and field are similar.

[44] S. Adachi, *Properties of AlGaAs* (INSPEC, London, UK, 1993).

[45] I. Strzalkowski, S. Joshi, and C. R. Crowell, Dielectric constant and its temperature dependence for GaAs, CdTe, and ZnSe, Appl. Phys. Lett. **28**, 350 (1976).

[46] Due to the competing effects of stronger near-field enhancement but higher thermal conductivity.

[47] P. R. West, S. Ishii, G. V. Naik, N. K. Emani, V. M. Shalaev, and A. Boltasseva, Searching for better plasmonic materials, Laser Photon. Rev. **4**, 795 (2010).

[48] A. Lalisse, G. Tessier, J. Plain, and G. Baffou, Quantifying the efficiency of plasmonic materials for near-field enhancement and photothermal conversion, J. Phys. Chem. C **119**, 25518 (2015).

[49] D. Ricard, P. Roussignol, and C. Flytzanis, Surface-mediated enhancement of optical phase conjugation in metal colloids, Opt. Lett. **10**, 511 (1985).

[50] S. T. Sundari, S. Chandra, and A. K. Tyagi, Temperature dependent optical properties of silver from spectroscopic ellipsometry and density functional theory calculations, J. Appl. Phys. **114**, 033515 (2013).

[51] It should be noted, however, that the exact values of the thermoderivatives are difficult to deduce from [50] because the permittivity values themselves can only extracted from a rather dense set of graphs.

[52] See an earlier version of this manuscript ([53], Sec. IV C).

[53] I. Gurwich and Y. Sivan, Metal nanospheres under intense continuous wave illumination—a unique case of non-perturbative nonlinear nanophotonics, arXiv:1702.03320.

[54] One can also numerically fit the results above [Figs. 1–4, panels (b)–(d)] with a second-order polynomial, i.e., to a cubic-quintic nonlinearity. However, such a pure fit cannot be linked directly to a specific physical effect (i.e., a thermoderivative), hence, will not provide clear physical insights. For that reason, we prefer the less accurate but physically meaningful approach.

[55] However, we note that the temperature-dependent ellipsometry studies reveal narrow spectral regimes where $B_m'' < 0$, e.g., for Au for $\lambda < 500$ nm (due to the effect of the Fermi smearing on the interband transitions [25,75]). This regime is, however, difficult to tune into resonance, in which case, the response of the system is expected to be weak. For Ag [50], a much narrower regime in which $B_m'' < 0$ around $\lambda = 400$ nm was identified but only for the lower-quality data of [50]. Even then, the thermoderivatives in this regime are much smaller than in all other cases. Yet, although elusive, such a regime is clearly highly desirable for plasmonic applications, since it gives rise to higher-quality factors and *stronger* fields.

[56] Obviously, $B_{\kappa,h}$ affects the field only at a higher order.

[57] J. B. Khurgin, G. Sun, W. T. Chen, W.-Y. Tsai, and D. P. Tsai, Ultrafast thermal nonlinearity, Sci. Rep. **5**, 17899 (2015).

[58] However, it should be noted that some of the conclusions drawn in [57] relied on inaccurate permittivity data. Specifically, the change of ϵ_m'' can reach many tens of percent, especially in the near-infrared regime studied in [57]; see [24,26,27,50], and is typically larger than that of the dielectric, see Sec. V A.

[59] We expect the shape to affect the nonlinear response as well; however, a quantification of this effect requires more exact numerical calculations that account for field and temperature nonuniformity; this will be performed in a future study.

[60] A. L. Tchebotareva, P. V. Ruijgrok, P. Zijlstra, and M. Orrit, Probing the acoustic vibrations of single metal nanoparticles by ultrashort laser pulses, Laser Photon. Rev. **4**, 581 (2010).

[61] Such an analysis is available for pulsed illumination; it was first performed in [13] for picosecond pulses; however, later studies, see especially [23] offered alternative modeling.

[62] S. Sadat, A. Tan, Y. J. Chua, and P. Reddy, Nanoscale thermometry using point contact thermocouples, Nano Lett. **10**, 2613 (2010).

[63] G. Kucsko, P. C. Maurer, N. Y. Yao, M. Kubo, H. J. Noh, P. K. Lo, H. Park, and M. D. Lukin, Nanometre-scale thermometry in a living cell, Nature **500**, 54 (2013).

[64] M. Mecklenburg, W. A. Hubbard, E. R. White, R. Dhall, S. B. Cronin, S. Aloni, and B. C. Regan, Nanoscale temperature mapping in operating microelectronic devices, Science **347**, 629 (2015).

[65] Y.-K. Tzeng, P.-C. Tsai, H.-Y. Liu, O. Y. Chen, H. Hsu, F.-G. Yee, M.-S. Chang, and H.-C. Chang, Time-resolved luminescence nanothermometry with nitrogen-vacancy centers in nanodiamonds, Nano Lett. **15**, 3945 (2015).

[66] K. Kim, B. Song, V. Fernández-Hurtado, W. Lee, W. Jeong, L. Cui, D. Thompson, J. Feist, M. T. Homer Reid, F. J. García-Vidal, J. C. Cuevas, E. Meyhofer, and P. Reddy, Radiative heat transfer in the extreme near field, Nature **528**, 387 (2015).

[67] J. T. Hugall and J. J. Baumberg, Demonstrating photoluminescence from Au is electronic inelastic light scattering of a plasmonic metal: The origin of SERS backgrounds, Nano Lett. **15**, 2600 (2015).

[68] L. Sarkhosh and N. Mansour, Study of the solution thermal conductivity effect on nonlinear refraction of colloidal gold nanoparticles, Laser Phys. **25**, 065404 (2015).

[69] O. Neumann, A. S. Urban, J. Day, S. Lal, P. Nordlander, and N. J. Halas, Solar vapor generation enabled by nanoparticles, ACS Nano **7**, 42 (2013).

[70] Z. Fang, Y. R. Zhen, O. Neumann, A. Polman, F. J. Garcia de Abajo, P. Nordlander, and N. J. Halas, Evolution of light-induced vapor generation at a liquid-immersed metallic nanoparticle, Nano Lett. **13**, 1736 (2013).

[71] D. Boyer, P. Tamarat, A. Maali, B. Lounis, and M. Orrit, Photothermal imaging of nanometer-sized metal particles among scatterers, Science **297**, 1160 (2002).

[72] V. P. Zharov and D. O. Lapotko, Photothermal imaging of nanoparticles and cells, IEEE J. Sel. Top. Quantum Electron. **11**, 733 (2005).

[73] A. Danielli, K. Maslov, A. Garcia-Uribe, A. M. Winkler, C. Li, L. Wang, Y. Chen, G. W. Dorn, and L. V. Wang, Label-free photoacoustic nanoscopy, J. Biomed. Opt. **19**, 086006 (2014).

[74] V. P. Zharov, Ultrasharp nonlinear photothermal and photoacoustic resonances and holes beyond the spectral limit, Nat. Photon. **5**, 110 (2011).

[75] P. Winsemius, M. Guerrisi, and R. Rosei, Splitting of the interband absorption edge in Au: Temperature dependence, Phys. Rev. B **12**, 4570 (1975).